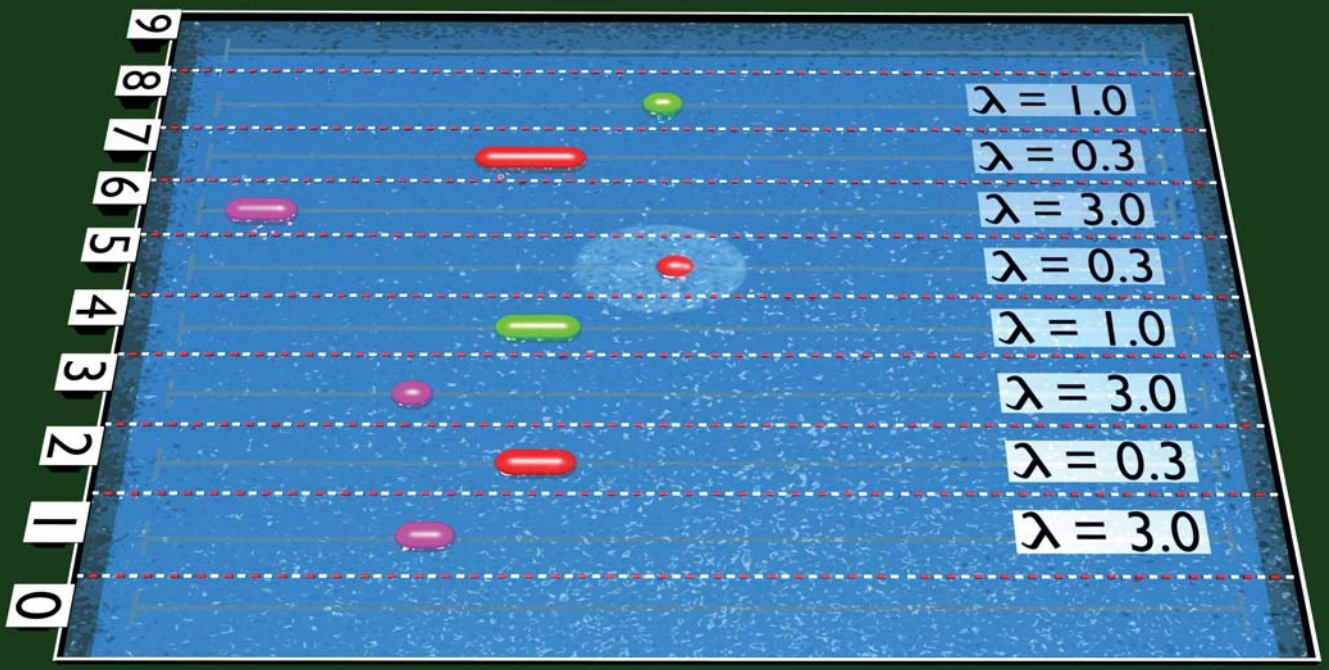

Featuring work from the group of Prof. Piotr Garstecki at the Institute of Physical Chemistry, Polish Academy of Sciences, Warsaw, Poland.

Title: Speed of flow of individual droplets in microfluidic channels as a function of the capillary number, volume of droplets and contrast of viscosities.

Automated measurements of the speed of droplets in microfluidic channels reveal complex dependencies on a range of parameters and guide the use of droplets in analytical applications. Project operated within the Foundation for Polish Science Team Programme co-financed by the European Regional Development Fund.

As featured in:

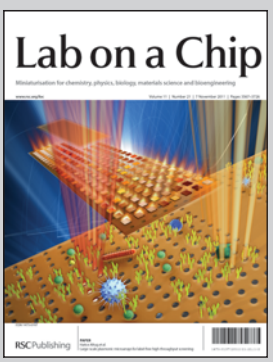

See Piotr Garstecki *et al.*, *Lab Chip*, 2011, **11**, 3603.

RSC Publishing

www.rsc.org/loc

Registered Charity Number 207890

Lab on a Chip

Dynamic Article Links

Cite this: *Lab Chip*, 2011, **11**, 3603

www.rsc.org/loc

PAPER

Speed of flow of individual droplets in microfluidic channels as a function of the capillary number, volume of droplets and contrast of viscosities

Slawomir Jakiela,[a] Sylwia Makulska,[a] Piotr M. Korczyk[ab] and Piotr Garstecki*[a]

Received 17th June 2011, Accepted 11th August 2011
DOI: 10.1039/c1lc20534j

Droplet microfluidic techniques offer an attractive compromise between the throughput (of *i.e.* reactions per second) and the number of input/output controls needed to control them. Reduction of the number of controls follows from the confinement to essentially one-dimensional flow of slugs in channels which—in turn—relies heavily on the speed of flow of droplets. This speed is a complicated function of numerous parameters, including the volume of droplets (or length L of slugs), their viscosity μ_d, viscosity μ_c and rate of flow of the continuous phase, interfacial tension and geometry of the cross-section of the channel. Systematic screens of the impact of these parameters on the speed of droplets remain an open challenge. Here we detail an automated system that screens the speeds of individual droplets at a rate of up to 2000 experiments per hour, with high precision and without human intervention. The results of measurements in channels of square cross-section (of width $w = 360$ μm) for four different values of the contrast of viscosities $\lambda = \mu_d/\mu_c = 0.3$, 1, 3, and 33, wide ranges of values of the capillary number $Ca \in (10^{-4}, 10^{-1})$, and wide ranges of lengths of droplets $l = L/w \in (0.8, 30)$ show that the speed of droplets depends significantly both on l and on λ. The dependence on Ca is very strong for $\lambda > 1$, while it is less important both for $\lambda \leq 1$ and for $\lambda \gg 1$.

Compartmentalization of reactions into droplets brings in a range of benefits. Bulk emulsion techniques take advantage of the increased ratio of surface to volume that facilitates interphase transfer. These techniques offer virtually any throughput but are completely incapable of addressing and manipulating individual droplets. Such manipulation can be used in high throughput screens to perform a large number of *different* reactions in small compartments, *i.e.* on small volumes of reagents. For example, digital platforms[1–3] offer the individual and simultaneous control of each droplet at the expense of the large number of input/output controls needed to address each electrode in the array. Droplet microfluidic chips offer an attractive compromise between the throughput and the number of controls. In such systems droplets are formed and transported in channels sequentially. Highly reproducible generation of droplets[4–7] in passive systems, or controlled formation of droplets on demand,[8–13] *i.e.* with individually prescribed volumes at individually prescribed times of emission, can be used to screen[8,14,15] conditions of reactions or incubations with the use of only a few i/o channels.

Droplet microfluidics has been demonstrated to provide attractive solutions in a wide range of applications from synthesis of nanomaterials to *in vitro* expression of genes and incubation of bacteria.[16–18] Recently droplet microfluidics has been continually developed towards controlling the flow of droplets in networks[19–22] and towards automation enabling synchronization of packets of droplets for formation of sequences of reaction mixtures,[8] incubation over predetermined intervals and sorting.[23,24]

All droplet microfluidic techniques rely on transport of droplets in channels. Thus characterization and—ultimately—understanding of the relation between the speed of flow of droplets and the numerous parameters that influence this flow are important. This forms a formidable challenge because the number of parameters is large, including viscosities of both phases, interfacial tension, volume of droplets, geometry of the channel, speed of flow of the continuous liquid, presence, type and concentration of surfactants and because—as we demonstrate here—the spectrum of behaviours is rich.

For these reasons, in spite of the apparent simplicity and starkly clear definition of the problem (*i.e.* what is the speed of a droplet given the well defined parameters), characterization of phenomenology and understanding of the mechanisms behind them remain elusive. The difficulty is well reflected in the apparent scatter of recent experimental results on the subject. For example, Fuerstman *et al.*[25] monitored the motion of bubble trains in channels of rectangular cross-sections (20–75) μm × (68–132) μm and found that in the absence of surfactants the speed of bubbles u_d is equal to the mean speed u_c of the

[a]*Institute of Physical Chemistry, Polish Academy of Sciences, Kasprzaka 44/52, 01-224 Warsaw, Poland*
[b]*Institute of Fundamental Technological Research, PAS, Pawińskiego 5B, 02-106 Warsaw, Poland. E-mail: garst@ichf.edu.pl*

continuous liquid, *i.e.* the mobility $\beta = u_d/u_c = 1$. Surprisingly, the small concentration of the surfactant lowered the value of β to ~0.48, while the large concentration of the surfactant resulted in $\beta \approx 0.83$. In another work, Vanapalli *et al.*[26] used a system that had two channels (each of cross-section of 200 × 120 μm) interconnected downstream of the test section. A single droplet introduced into the test section modified the hydraulic resistance of one of the channels and changed the distribution of flow at the junction downstream, allowing for measurement of the contribution r_d of the droplet to the hydraulic resistance of the channel. Vanapalli *et al.* found $\beta = 1.28$ for all droplets that they tested ($L/w \in (1.5, 7.2)$ and $\lambda = 0.03$ and 0.88) independent of the value of $Ca \in (10^{-3}, 10^{-2})$. In a stark contrast, Labrot *et al.*[27] measured $\beta = 1.6$ for $Ca \in (10^{-3}, 4 \times 10^{-3})$, $\lambda \in (1/20, 70)$ in a rectangular channel (500 × 300 μm) for droplet trains. In another experiment Sessoms *et al.*[28] studied small periodic droplet trains and found $\beta > 1$ for $l < 1$ and $\beta < 1$ for drops larger than the width of the channel.

The scope of analytical predictions is also quite limited. Taylor[29] considered the problem of flow of a semi-infinite single bubble in a capillary. He found that the ratio m of the cross-section of the capillary occupied by the liquid deposited on the walls is proportional to $Ca^{1/2}$, with $Ca = \mu_c u_b/\gamma$. Since the finger of air (propagating at speed u_b) pushes liquid at a rate $(1 - m)Au_b$ (A representing the area of cross-section of the capillary), the average speed of liquid in front of the finger is $u_c = (1 - m)u_b$ yielding $\beta = u_b/u_c = (1 - m)^{-1}$.

The motion of a finite single bubble in a circular capillary was studied by Bretherton[30] who found m (which he called W) proportional to $Ca^{2/3}$. Schwartz *et al.*[31] confirmed Bretherton's results in the case of long single bubbles and introduced corrections to the scaling for short ones.

A *viscous* droplet in a circular capillary was analyzed first by Hodges *et al.*[32] who found that the thickness ε of the film of the continuous liquid between the droplet and the wall of the capillary scales with the same exponent (2/3) of the capillary number as predicted by Bretherton, but that there is a multiplying factor of small magnitude depending both on Ca and λ.

Most relevant to microfluidic systems are capillaries of the rectangular cross-section. Wong *et al.*[33,34] considered analytically the flow of single finite bubbles in *polygonal* ducts. In such ducts, the continuous liquid can flow by the bubble or droplet much easier than in the case of capillaries of the circular cross-section. This is because the interfacial tension does not allow the bubble/droplet to fill the corners of the capillary (as this would induce a large radial curvature of the interface). These corners act as 'gutters' for the continuous liquid. Wong *et al.* have shown *via* modeling that for very small values of the capillary number ($Ca < 10^{-6}$) the flow through the gutters dominates, yielding a pressure drop along the bubble being proportional to Ca. For larger values of Ca plug flow dominates and the pressure drop is proportional to $Ca^{2/3}$, as was earlier found for circular capillaries.

The results that we present below cannot be described by any existing theory and clearly demonstrate the rich variety of functional forms of the dependence of the speed of droplets on relevant parameters. These results may have important practical implications because the speed of the droplets may significantly depend (i) on their length, especially when the viscosity of the droplet liquid is larger than that of the continuous liquid, (ii) on the value of the capillary number, in a complicated and non-monotonic way, and (iii) on the ratio of viscosities of the two immiscible liquids.

Methods

Experimental system

We designed the experimental system with the following objectives in mind: (i) to minimize the need for human intervention during measurements, (ii) to minimize the fluctuations of the temperature of the liquids and the system, and (iii) to optimize for minimum uncertainty of measurements against possibly high rate of screening of the parameters.

The schematics of the system is depicted in Fig. 1. In short, a T-junction chip was placed on a stereoscope equipped with a fast linear camera. The chip was supplied with liquids from pressurized reservoirs *via* electromagnetic valves. Camera, thermocouple probe, electronic proportional regulator, electromagnetic valves and digital manometers were connected to appropriate I/O National Instruments cards (NI PCIE-6320, NI PCI-6703 and NI PCIE-1429). Custom written Lab View software allowed us to: (i) control the pressure of the continuous liquid, (ii) monitor the pressures of both liquids together with the temperature at the chip, (iii) create droplets on demand *via* steering of the two electromagnetic valves, (iv) analyze images acquired from the camera in real time (at 70 kHz) and (v) extract the speed and length of the droplets.

We enclosed all the parts that did not require manual regulation in a box made of polycarbonate. A thermocouple probe (Pt100) reported the temperature T on the chip to the computer. We found that T was stable at 25 °C within ±0.6 °C during all experiments, provided that the system was first turned on and allowed to equilibrate for ~45 minutes.

The liquids

In all experiments we used hexadecane (Alfa Aesar, as supplied) as the continuous liquid. We measured the viscosity

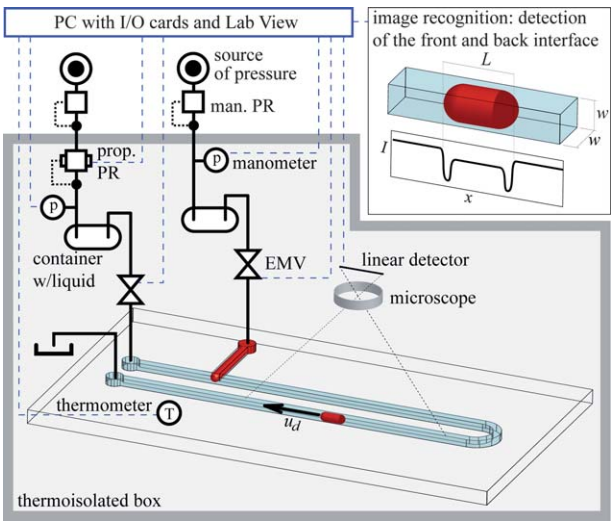

Fig. 1 Schematic diagram of the experimental system. For explanation refer to the text. Meaning of abbreviations: man.—manual, prop.—proportional, PR—pressure regulator, EMV—electromagnetic valve.

$\mu_c = 3.0 \pm 0.1$ mPa s and density $\rho_c = 770$ kg m^{-3} at 25 °C. For the droplet liquid we used distilled water (Millipore, viscosity $\mu_d = 0.890$ mPa s, interfacial tension with hexadecane $\gamma = 46.1 \pm 1.6$ mN m^{-1}, density $\rho_d = 997$ kg m^{-3} and the static contact angle for hexadecane–water–PC $\phi_d = 125 \pm 1.8°$ at 25 °C) and water–glycerine solutions with different contents of glycerine: (i) 38.2% (w/w) solution of glycerine in water of viscosity $\mu_d = 3.03 \pm 0.1$ mPa s, interfacial tension $\gamma = 27.1 \pm 0.7$ mN m^{-1}, density $\rho_d = 1092$ kg m^{-3} and $\phi_d = 142.3 \pm 1.3°$ at 25 °C, (ii) 61.5%, $\mu_d = 10.1 \pm 0.3$ mPa s, $\gamma = 25.4 \pm 0.6$ mN m^{-1}, $\rho_d = 1155$ kg m^{-3} and $\phi_d = 131 \pm 2.1°$ at 25 °C and (iii) 86.3%, $\mu_d = 99.6 \pm 0.8$ mPa s, $\gamma = 30.2 \pm 0.8$ mN m^{-1}, $\rho_d = 1222$ kg m^{-3} and $\phi_d = 114 \pm 1.9°$ at 25 °C. We measured the interfacial tensions using the pendant droplet method, averaging over 10 independent measurements. We measured the viscosities of the liquids by passing them through a resistive steel capillary at 25 °C and under a pressure head of 500 mbar and calibrating the results with those obtained for water, for which we assumed the value of viscosity from the literature.

We took care not to incorporate any surface active agents into the liquids. Before every exchange of the liquids, we washed the containers with isopropanol, distilled water and compressed air.

The chip

We used a T-junction system micro-milled in polycarbonate (PC) and bonded with a flat slab of PC.[35] The cross-section of all the channels were $A = w^2 = 360 \pm 7 \times 360 \pm 7$ μm^2. We modified the surface of the walls of the channels with dodecylamine[35] to guarantee complete wetting of the walls by hexadecane. After the procedure of surface modification we thoroughly rinsed the channels (by passing hexadecane for several hours) to ensure that no remains after the modification procedure could farther dissolve into the continuous phase.

Supply of liquids

We controlled the pressure p_d applied to the reservoir of the droplet liquid with a manual pressure regulator (Rexroth PR1-RGP). The liquid flew from the reservoir into an electromagnetic valve (EMV$_d$) and a resistive steel capillary (O.D. 400 μm, I.D. 205 μm, length = 2 m, Mifam, Poland), as described by Churski *et al.*[8] We delivered the continuous liquid from another pressurized container, with the pressure p_c ranging between 0.1 bar and 8 bar and controlled with an electronic proportional regulator (Parker, MPT 40) steered from the computer. We used a set of capillaries of different lengths (from 10 cm to 200 cm) to regulate[36] the range of rates of flow Q_c available *via* tuning of p_c. The total range of Q_c was 1 to 800 mL h^{-1}, corresponding to Ca $\in (10^{-4}, 10^{-1})$. The fluctuations of p_c were less than ±3 mbar in all experiments. Both before and after each series of experiments we calibrated the dependence $Q_c(p_c)$ by weighing liquid flowing out from the chip onto a balance (WLC-C/2, Radwag). We estimate the error of the calibration of $Q_c(p_c)$ to be within ±0.1% of the fitted relation.

Formation of droplets

Formation of droplets on demand was described earlier.[8] Here we used pre-calibrated scripts that formed droplets of lengths ranging from 0.8 to 30 w (~50 to 1500 nL in volume).

Measurement of the length and speed of the droplets

We used a stereoscope (Nikon SMZ 1500) equipped with a linear camera (AViiVA II EM4 CL 2014, E2V) that acquires images at 70 kHz and reports them in real time to the computer. We focused the camera at the centreline of the microchannel. The 2048 pixel sensor acquired light from a 2 cm long section of the channel yielding 10 μm of resolution in space and 15 μs of resolution in time.

We measured the speed of droplets in a section of the channel that was ~10 cm downstream of the T-junction to ensure that the measurement is conducted at a stationary state of flow (*i.e.* the flow is fully developed and no longer perturbed by the process of formation of droplet). To further confirm stability of flow we checked the speed of droplets for a few values of capillary numbers for different positions (~15 cm and ~20 cm) downstream of the T-junction. The results were the same. The speed of each droplet was estimated by the ratio of the fixed distance of 2 cm covered by the linear camera to the interval between entering and leaving this section by the front of the droplet. We estimate the error of measurement of the speed to be less than 1%.

We measured the lengths of the droplets by analyzing the signal from the linear camera. The fore- and rear-caps of the droplets produced clearly distinguishable negative peaks in the intensity recorded by the camera. We found Poisson distribution to fit these troughs best and used this distribution in all experiments. We calibrated this measurement *via* a series of experiments in which we recorded the image of the droplets simultaneously on the linear camera and with a standard 2D CMOS chip (uEye, USB UI-1460SE). We estimate the error in the measurement of the length of the droplet to be below 2%.

For some series of data we also measured the static lengths (l_s) of the droplets by first forming a droplet, advancing it slightly from the junction, stopping the flow, measuring l_s, and then opening the flow to measure the dynamic length (l_d). Fig. 2 shows that all droplets elongated in flow. Interestingly, the surplus length (*i.e.* $l_d - l_s$) increased with l_s up to the maximum value. We can speculate that perhaps the optimum (*i.e.* minimizing dissipation) shape of the caps has a finite length and droplets that are too short cannot acquire this optimum. It is, however, puzzling that for $l_s > 5$ the surplus length decreased with increasing l_s for very long slugs.

As $(l_d - l_s)/l_s$ was small (less than 10%) in order to maximize the rate of experiments, in all the subsequent measurements of the speed we only monitored the dynamic length (which we mark as l for brevity).

Experiments

We performed the experiments in series. Each series was done for a given set of liquids (*i.e.* for a fixed value of λ) and for a fixed value of the capillary number (*i.e.* for a fixed speed of flow of the continuous liquid). Within the series the computer automatically screened the whole range of volumes of droplets, corresponding to the length of the slugs $l/w = 1$ to 30 changed in steps of ~0.5 or more. For each volume of the droplet the computer performed at least ten repetitions to ensure reproducibility and acquire sufficient statistics. In each experiment the system formed a *single* droplet and then monitored the speed u_d.

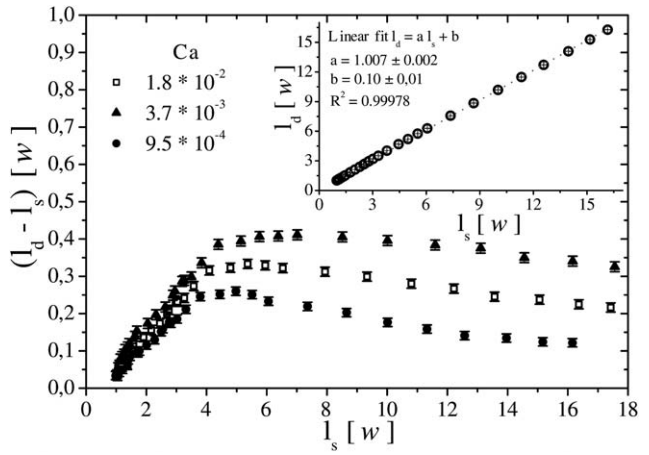

Fig. 2 Illustration of the difference between the dynamic length (*i.e.* length measured during flow) and the static length (measured at rest) of droplets of water in hexadecane. The dynamic measurements were taken for three values of Ca: 9.5×10^{-4}, 3.7×10^{-3} and 1.8×10^{-2}. The inset shows the quality of the simplified linear correlation between the dynamic and static length for Ca = 9.5×10^{-4}.

In addition, we repeated each series of measurements three times and (within this number) at least once on a different day to ensure reproducibility of the data. We also checked for consistency of the measurements by running the same screens on a separately prepared copy of the microfluidic system. The data that we present below are averages of the three repetitions (*i.e.* each data point is an average of about 30 independent measurements and the error bars are given by the standard deviation of the set).

Results

$\lambda = 1$. We first show the results of the screens of the speed of droplets of a 38.2% (w/w) solution of glycerine in water of viscosity $\mu_d = 3.03$. The contrast of viscosities is $\lambda = (3.03/3.0) \approx 1$. We graphed the coefficient of speed β in Fig. 3. Small droplets ($l < 2$) flow faster than the mean speed of the continuous liquid. The smallest droplets that we tracked ($l \approx 1.3$) flew significantly faster than u_c ($\beta = 1.26$), in spite of the fact that these droplets are already large enough to be effectively confined by the channels ($l > 1$).

For longer droplets we observe a minimum in β at a value of few percent below unity for $l \approx 3$, a maximum in β at a value of unity or few percent above for $l \in$ (11.5–13.5) and then a gradual decrease of β with increasing l down to values few percent below 1. The values of β at these extrema depend on the value of Ca. At Ca = 5.2×10^{-4} $\beta_{min} \approx 0.985$, then as Ca increases the minimum gets deeper ($\beta_{min} \approx 0.97$ at Ca = 6.7×10^{-3}), and then, with further increase of the speed of flow of the continuous liquid, the minimum gets shallower again ($\beta_{min} \approx 0.98$ at Ca = 1.1×10^{-1}). The maximum value of β_{max} for $l \in$ (11.5, 13.5) increases monotonically from $\beta_{max} \approx 1.00$ at Ca = 5.2×10^{-4} to $\beta_{max} \approx 1.02$ at Ca = 1.1×10^{-1}. Finally, for very long droplets β decreases to a value that is almost equal to unity ($\beta \approx 0.99$ at Ca = 5.2×10^{-4}) to smallest values for the largest capillary number that we tested ($\beta \approx 0.96$ at Ca = 1.1×10^{-1}).

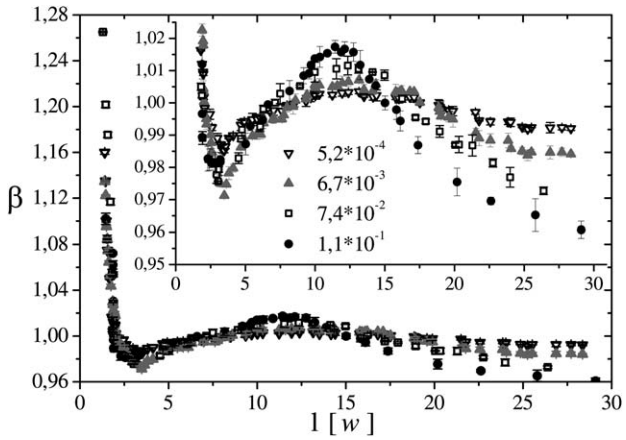

Fig. 3 Graph of the coefficient of mobility of droplets $\beta = u_d/u_c$ as a function of the length of the droplet $l = L/w$ for a range of values of the capillary number (listed in the figure) and for the contrast of viscosities $\lambda = \mu_d/\mu_c = 1$. Each point represents an average of ~30 measurements and the error bars are given by the standard deviation within this set.

$\lambda = 0.3$. In order to probe the speeds of droplets that are less viscous than the continuous phase we used distilled water of viscosity $\mu_d = 0.890$ mPa s, resulting in $\lambda = 0.89/3.0 = 0.3$. We graphed the results in Fig. 4. Small droplets behave similarly to the case of $\lambda = 1$, *i.e.* they flow significantly faster (up to 40% in our measurements) than the mean speed of oil, even when $l > 1$. For larger l the mobility β decreases to cross the value of 1 for $l =$ ~1.7 to ~2, depending on the value of Ca. Even longer droplets flow slightly slower than the mean speed of oil: β decreases with increasing λ down to a minimum value of few percent below unity, and then increases again asymptotically to unity. The maximum in β observed for $\lambda = 1$ was absent for $\lambda = 0.3$.

Interestingly, as we described in detail previously,[37] the minimum value of mobility (β_{min}) shows a discontinuity in its evolution with increasing capillary number. At smallest values of Ca = 1.5×10^{-4}, $\beta_{min} = 0.98$, and increases with increasing Ca to $\beta_{min} \approx 1$ (without a minimum and only an asymptotic approach to unity from above for Ca = 8×10^{-4}). For slightly larger values

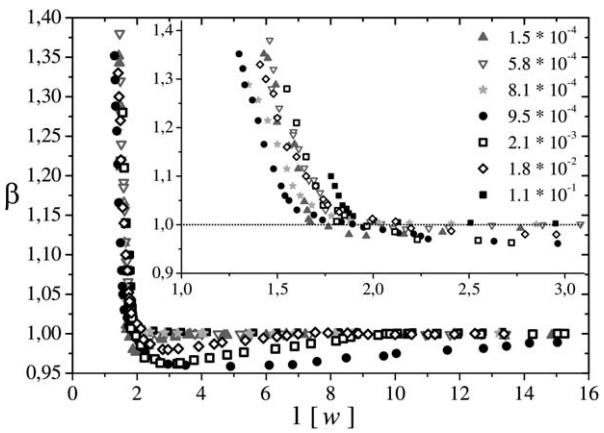

Fig. 4 Graph of the coefficient of mobility of droplets $\beta = u_d/u_c$ as a function of the length of the droplet $l = L/w$ for a range of values of the capillary number (listed in the figure) and for the contrast of viscosities $\lambda = \mu_d/\mu_c = 0.3$. Each point represents an average of ~30 measurements. We did not plot the error bars for clarity of the graph.

of Ca the minimum reappeared deeper ($\beta_{min} = 0.95$) to get gradually more shallow again with increasing Ca. This cross-over is associated with a change of the topology of flow inside the droplet: at the transition convective rolls that are present in the continuous liquid in front and behind the droplet enter the droplet.

From a practical point of view, the speed of droplets in these two systems ($\lambda = 0.3$ and $\lambda = 1$) is quite simple—small droplets travel faster than the continuous liquid yet for droplets longer than *ca.* two widths of the channel, the speed is almost (to within 5%) equal to the superficial speed of oil, regardless of value of the capillary number.

$\lambda > 1$. When droplets are more viscous than the continuous liquid the dependence of the speed of droplets on their length and on Ca is quite different from the cases described above (Fig. 5). We found that droplets of 61.5% solution of glycerine in water ($\mu_d = 10.1$, $\lambda = 3.37$) *always* flew slower than the mean speed of the flow of oil. Unlike the cases of all the other values of λ that we tested, even small droplets ($l < 2$) presented mobilities $\beta < 1$. Further, and again in contrast to all other values of λ, we found that β initially increased with increasing l, to reach a maximum, and then to decrease with increasing l, probably to saturate at a fixed value (this saturation is best visible for the smallest Ca = 4.2×10^{-4} that we tested). The position of the maximum changed with the value of Ca, from $l \approx 1.5$ (at Ca = 4.2×10^{-4}) to $l \approx 4.5$ (at Ca = 3.3×10^{-2}). For this contrast of viscosities the mobility β depended most strongly both on l and on Ca. For example, droplets of length $l = 4$ presented $\beta = 0.72$ for Ca = 4.2×10^{-4} and $\beta = 0.92$ for Ca = 3.3×10^{-4}. Similarly, at Ca = 7.2×10^{-3} droplets of length $l = 6$ presented $\beta = 0.86$, and those of length $l = 10$ presented $\beta = 0.68$.

$\lambda \gg 1$. We also tested the case in which droplets were significantly more viscous than the continuous liquid. We used the 86.3% solution of glycerine in water of viscosity $\mu_d = 99.6$ mPa s, resulting in $\lambda = 33.2$ (Fig. 6). The results are surprisingly—in comparison to the ones presented above—simple: the curves $\beta(l)$ fall onto a single master line for all values of Ca $\in$ (3.5×10^{-4}, 1.1×10^{-1}). It is also quite surprising, in view of the results for $\lambda = 3.32$ that small droplets ($l < \sim 4.5$) flow faster than the mean speed of the continuous liquid.

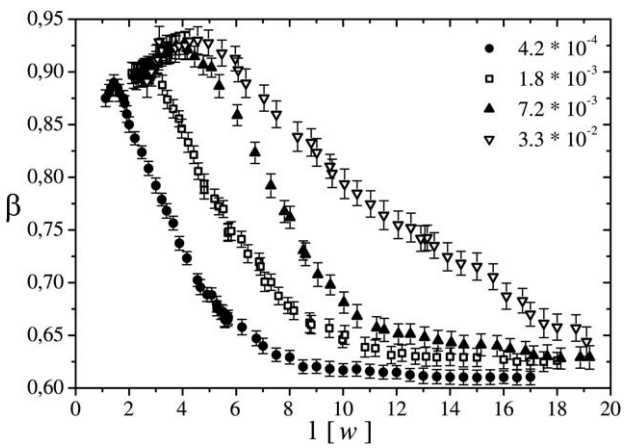

Fig. 5 Graph of the coefficient of mobility of droplets $\beta = u_d/u_c$ as a function of the length of the droplet $l = L/w$ for a range of values of the capillary number (listed in the figure) and for the contrast of viscosities $\lambda = \mu_d/\mu_c = 3$. Each point represents an average of ~30 measurements and the error bars are given by the standard deviation within this set.

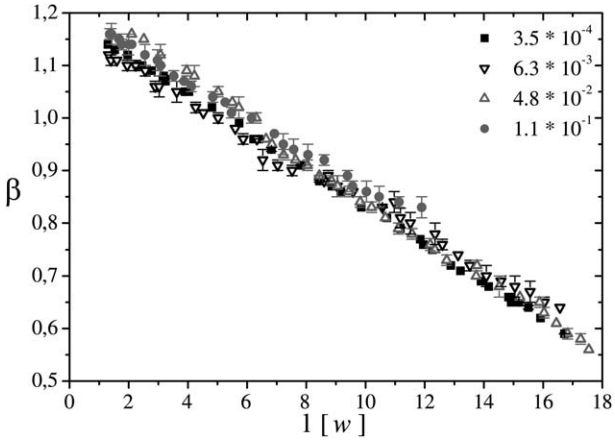

Fig. 6 Graph of the coefficient of mobility of droplets $\beta = u_d/u_c$ as a function of the length of the droplet $l = L/w$ for a range of values of the capillary number (listed in the figure) and for the contrast of viscosities $\lambda = \mu_d/\mu_c = 33.2$. Each point represents an average of ~30 measurements and the error bars are given by the standard deviation within this set.

Discussion

The results that we described above clearly show that the speed of droplets is a complicated function that depends significantly on a number of parameters. In selected ranges of parameters the dependence of speed on the value of capillary number alone is strong, in others it is weak.

The value of the contrast of viscosities of the two phases has a significant influence on the speed of droplets. At small values of the contrast ($\lambda \leq 1$) the mobilities of droplets deviate significantly from unity only for short droplets. For larger viscosities of the droplet liquid their mobility depends significantly both on the value of the capillary number and on the length of the droplet.

Fig. 7 shows the mobility β of droplets in selected ranges of the length of the droplet (small droplets $l < 2$, droplets that are most convenient for performing reactions within them $l \in$ (2, 5) and

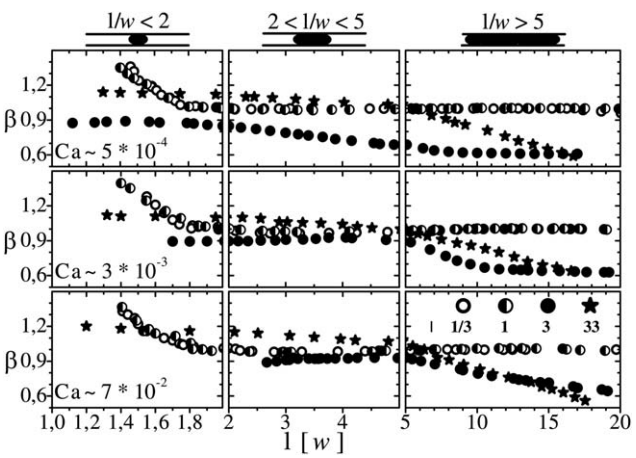

Fig. 7 Comparison of the relations $\beta(l, \lambda)$ for three different ranges of the length of the droplets (short, medium and long) for three values of the capillary number.

long slugs $l > 5$), for three different values of the capillary number: Ca $\approx 10^{-4}$, 10^{-3} and 10^{-2} (the exact values of Ca are different for different values of λ and are given in the figure).

Small droplets ($l < 2$) are faster than the mean speed of flow for all values of Ca and λ with the exception of $\lambda = 3$. The medium length droplets $l \in (2, 5)$ in most cases present mobilities $\beta \approx 1$ within a few percent. The exceptions include $\lambda = 3$ at smallest values of Ca $\approx 10^{-4}$ for which parameters $\beta < 0.85$, and $\lambda = 33.2$ at largest values of Ca $\approx 10^{-4}$ when $\beta > 1.1$. The speed of flow of long slugs depends significantly on the value of the contrasts of viscosities. For $\lambda \leq 1$ the mobility of these long droplets is equal to 1 for all values of Ca. For greater values of λ the value of β depends significantly both on the length of the slug and on the value of Ca and is generally significantly less than one.

Conclusions

The results presented above show quite a complex landscape of functional dependence of the mobility of droplets on the values of parameters, especially on the value of the capillary number. Still, it is possible to draw certain simple conclusions of practical importance. For example, when the droplet liquid is less viscous than the continuous liquid the speed of slugs longer than *ca.* two times the width of the channel is equal to the superficial speed of the continuous liquid to within few percent. Thus, in all applications that do not require precise synchronization or precise timing of *e.g.* incubation intervals, the speed of droplets can be assumed to equal the average speed in the channel. On the other hand, when the droplet liquid is more viscous than the continuous phase—as might be the case for *e.g.* droplets containing physiological liquids—the mobility of the droplets cannot be assumed to be equal to one, even in imprecise applications. Also in applications in which long sequences of droplets are flowing through a channel or tubing even small differences in β for different lengths of the droplets may lead to systematic changes in the intervals between droplets, or even to merging of drops.

It is important to keep in mind that all the results presented and discussed above are obtained in channels of square cross-sections in which single droplets were considered in the absence of surfactants. Both the aspect ratio of the width to height of the channel and the presence of surface active agents may introduce significant changes to the value and functional form of β (Ca, l, λ). It is quite clear that further experimental research is needed to characterize these dependencies and perhaps prompt and facilitate construction of an analytical understanding of the physics of motion of droplets in rectangular channels. Ultimately, a range of applications of droplet microfluidic systems (especially those using either physiological liquids or *e.g.* liquid media for cell growth) would benefit greatly from a compact model predicting the value of β as a function of the relevant parameters. We hope that the use of automated systems similar to the one reported here will help to generate the necessary data to construct, at least, an empirical model.

Acknowledgements

Project operated within the Foundation for Polish Science Team Programme co-financed by the EU European Regional Development Fund.

Notes and references

1 R. B. Fair, *Microfluid. Nanofluid.*, 2007, **3**, 245–281.
2 N. R. Beer, B. J. Hindson, E. K. Wheeler, S. B. Hall, K. A. Rose, I. M. Kennedy and B. W. Colston, *Anal. Chem.*, 2007, **79**, 8471–8475.
3 N. R. Beer, E. K. Wheeler, L. Lee-Houghton, N. Watkins, S. Nasarabadi, N. Hebert, P. Leung, D. W. Arnold, C. G. Bailey and B. W. Colston, *Anal. Chem.*, 2008, **80**, 1854–1858.
4 S. L. Anna, N. Bontoux and H. A. Stone, *Appl. Phys. Lett.*, 2003, **82**, 364–366.
5 T. Thorsen, R. W. Roberts, F. H. Arnold and S. R. Quake, *Phys. Rev. Lett.*, 2001, **86**, 4163–4166.
6 P. Garstecki, M. J. Fuerstman, H. A. Stone and G. M. Whitesides, *Lab Chip*, 2006, **6**, 437–446.
7 P. Garstecki, H. A. Stone and G. M. Whitesides, *Phys. Rev. Lett.*, 2005, **94**, 164501.
8 K. Churski, P. Korczyk and P. Garstecki, *Lab Chip*, 2010, **10**, 816–818.
9 K. Churski, J. Michalski and P. Garstecki, *Lab Chip*, 2010, **10**, 512–518.
10 A. Bransky, N. Korin, M. Khoury and S. Levenberg, *Lab Chip*, 2009, **9**, 516–520.
11 B. C. Lin and Y. C. Su, *J. Micromech. Microeng.*, 2008, **18**, 115005.
12 W. Wang, C. Yang and C. M. Li, *Lab Chip*, 2009, **9**, 1504–1506.
13 J. Xu and D. Attinger, *J. Micromech. Microeng.*, 2008, **18**, 065020.
14 B. Zheng, L. S. Roach and R. F. Ismagilov, *J. Am. Chem. Soc.*, 2003, **125**, 11170–11171.
15 X. Niu, F. Gielen, J. B. Edel and A. J. deMello, *Nat. Chem.*, 2011, **3**, 437–442.
16 V. Taly, B. T. Kelly and A. D. Griffiths, *ChemBioChem*, 2007, **8**, 263–272.
17 L. M. Fidalgo, G. Whyte, D. Bratton, C. F. Kaminski, C. Abell and W. T. S. Huck, *Angew. Chem., Int. Ed.*, 2008, **47**, 2042–2045.
18 H. Song, D. L. Chen and R. F. Ismagilov, *Angew. Chem., Int. Ed.*, 2006, **45**, 7336–7356.
19 M. J. Fuerstman, P. Garstecki and G. M. Whitesides, *Science*, 2007, **315**, 828–832.
20 M. Prakash and N. Gershenfeld, *Science*, 2007, **315**, 832–835.
21 F. Jousse, R. Farr, D. R. Link, M. J. Fuerstman and P. Garstecki, *Phys. Rev. E: Stat., Nonlinear, Soft Matter Phys.*, 2006, **74**, 036311.
22 O. Cybulski and P. Garstecki, *Lab Chip*, 2010, **10**, 484–493.
23 J. C. Baret, V. Tally, M. Ryckelynck, C. A. Merten and A. D. Griffiths, *Med Sci(Paris)*, 2009, **25**, 627–632.
24 O. J. Miller, K. Bernath, J. J. Agresti, G. Amitai, B. T. Kelly, E. Mastrobattista, V. Taly, S. Magdassi, D. S. Tawfik and A. D. Griffiths, *Nat. Methods*, 2006, **3**, 561–570.
25 M. J. Fuerstman, A. Lai, M. E. Thurlow, S. S. Shevkoplyas, H. A. Stone and G. M. Whitesides, *Lab Chip*, 2007, **7**, 1479–1489.
26 S. A. Vanapalli, A. G. Banpurkar, D. van der Ende, M. H. G. Duits and F. Mugele, *Lab Chip*, 2009, **9**, 982–990.
27 V. Labrot, M. Schindler, P. Guillot, A. Colin and M. Joanicot, *Biomicrofluidics*, 2009, **3**, 012804.
28 D. A. Sessoms, M. Belloul, W. Engl, M. Roche, L. Courbin and P. Panizza, *Phys. Rev. E: Stat., Nonlinear, Soft Matter Phys.*, 2009, **80**, 016317.
29 G. I. Taylor, *J. Fluid Mech.*, 1961, **10**, 161–165.
30 F. P. Bretherton, *J. Fluid Mech.*, 1961, **10**, 166–188.
31 L. W. Schwartz, H. M. Princen and A. D. Kiss, *J. Fluid Mech.*, 1986, **172**, 259–275.
32 S. R. Hodges, O. E. Jensen and J. M. Rallison, *J. Fluid Mech.*, 2004, **501**, 279–301.
33 H. Wong, C. J. Radke and S. Morris, *J. Fluid Mech.*, 1995, **292**, 95–110.
34 H. Wong, C. J. Radke and S. Morris, *J. Fluid Mech.*, 1995, **292**, 71–94.
35 D. Ogonczyk, J. Wegrzyn, P. Jankowski, B. Dabrowski and P. Garstecki, *Lab Chip*, 2010, **10**, 1324–1327.
36 P. M. Korczyk, O. Cybulski, S. Makulska and P. Garstecki, *Lab Chip*, 2011, **11**, 173–175.
37 S. Jakiela, P. Korczyk, S. Makulska and P. Garstecki, *Phys. Rev. Lett.*, 2011, submitted.

